Aqueous-phase reactive species formed by fine particulate matter from remote forest and polluted urban air

Haijie Tong[1,2*], Fobang Liu[1,3], Alexander Filippi[1], Jake Wilson[1], Andrea M. Arangio[1,4], Yun Zhang[5], Siyao Yue[6,7,8], Steven Lelieveld[1], Fangxia Shen[1,9], Helmi-Marja K. Keskinen[10,11], Jing Li[12], Haoxuan Chen[12], Ting Zhang[12], Thorsten Hoffmann[5], Pingqing Fu[8], William H. Brune[13], Tuukka Petäjä[10], Markku Kulmala[10], Maosheng Yao[12], Thomas Berkemeier[1], Manabu Shiraiwa[14], Ulrich Pöschl[1]

[1] Multiphase Chemistry Department, Max Planck Institute for Chemistry, 55128 Mainz, Germany
[2] Now at: Department of Civil and Environmental Engineering, The Hong Kong Polytechnic University, Kowloon, Hong Kong, China
[3] School of Chemical and Biomolecular Engineering, Georgia Institute of Technology, Atlanta, Georgia 30332, USA
[4] École Polytechnique Fédérale de Lausanne, Lausanne 1015, Switzerland
[5] Institute of Inorganic and Analytical Chemistry, Johannes Gutenberg University, 55128 Mainz, Germany
[6] State Key Laboratory of Atmospheric Boundary Layer Physics and Atmospheric Chemistry, Institute of Atmospheric Physics, Chinese Academy of Sciences, Beijing, 100029, China
[7] College of Earth and Planetary Sciences, University of Chinese Academy of Sciences, Beijing, 100049, China
[8] Institute of Surface-Earth System Science, Tianjin University, Tianjin, 300072, China
[9] School of Space and Environment, Beihang University, Beijing, 100191, China
[10] Institute for Atmospheric and Earth System Research / Physics, Faculty of Science, University of Helsinki, P.O. Box 64, FIN-00014, Helsinki, Finland
[11] Hyytiälä Forestry Field Station, Hyytiäläntie 124, FI-35500 Korkeakoski, Finland
[12] College of Environmental Sciences and Engineering, Peking University, Beijing, 100871, China
[13] Department of Meteorology, Pennsylvania State University, University Park, Pennsylvania 16802, USA
[14] Department of Chemistry, University of California, Irvine, California 92697-2025, USA

[*] *Correspondence to*: Haijie Tong (h.tong@mpic.de; haijie.tong@polyu.edu.hk)

Abstract

In the aqueous phase, fine particulate matter can form reactive species (RS) that influence the aging, properties, and health effects of atmospheric aerosols. In this study, we explore the RS yields of aerosol samples from remote forest (Hyytiälä, Finland) and polluted urban locations (Mainz, Germany; Beijing, China), and we relate the RS yields to different chemical constituents and reaction mechanisms. Ultrahigh-resolution mass spectrometry was used to characterize organic aerosol composition, electron paramagnetic resonance (EPR) spectroscopy with a spin-trapping technique was applied to determine the concentrations of $^{\bullet}OH$, $O_2^{\bullet-}$, and carbon- or oxygen-centered organic radicals, and a fluorometric assay was used to quantify H_2O_2. The aqueous H_2O_2-forming potential per mass unit of ambient $PM_{2.5}$ (particle diameter < 2.5 µm) was roughly the same for all investigated samples, whereas the mass-specific yields of radicals were lower for sampling sites with higher concentration of $PM_{2.5}$. The abundances of water-soluble transition metals and aromatics in ambient $PM_{2.5}$ were positively correlated with the relative fraction of $^{\bullet}OH$ and negatively correlated with the relative fraction of carbon-centered radicals. In contrast, highly oxygenated organic molecules (HOM) were positively correlated with the relative fraction of carbon-centered radicals and negatively correlated with the relative fraction of $^{\bullet}OH$. Moreover, we found that the relative fractions of different types of radicals formed by ambient $PM_{2.5}$ were comparable to surrogate mixtures comprising transition metal ions, organic hydroperoxide, H_2O_2, and humic or fulvic acids. The interplay of transition metal ions (e.g., iron and copper ions), highly oxidized organic molecules (e.g., hydroperoxides), and complexing or scavenging agents (e.g., humic or fulvic acids), leads to non-linear concentration dependencies in the aqueous-phase RS production. A strong dependence on chemical composition was also observed for the aqueous-phase radical yields of laboratory-generated secondary organic aerosols (SOA) from precursor mixtures of naphthalene and β-pinene. Our findings show how the composition of $PM_{2.5}$ can influence the amount and nature of aqueous-phase RS, which may explain differences in the chemical reactivity and health effects of particulate matter in clean and polluted air.

1 Introduction

Atmospheric fine particulate matter with a particle diameter < 2.5 µm ($PM_{2.5}$) can form reactive species (RS) upon dissolution in the aqueous phase (Bates et al., 2015;Lakey et al., 2016;Park et al., 2018;Li et al., 2018;Tong et al., 2019). The umbrella term RS comprises reactive oxygen species (e.g., $^{\bullet}OH$, $O_2^{\bullet-}$, $^1O_2$, H_2O_2, and ROOH) as well as C- and O-centered organic radicals (Halliwell and Whiteman, 2004;Sies et al., 2017), which influence the chemical aging of atmospheric aerosols and their interaction with the biosphere (Pöschl and Shiraiwa, 2015;Reinmuth-Selzle et al., 2017;Shiraiwa et al., 2017). For example, Fenton-like reactions of hydroperoxides with transition metal ions contribute to the formation of aqueous-phase radicals including $^{\bullet}OH$ (Jacob, 2000;Enami et al., 2014;Anglada et al., 2015;Tong et al., 2016a), enhancing the conversion of organic precursors to secondary organic aerosols (SOA) (Donaldson and Valsaraj, 2010;Ervens et al., 2011;Gligorovski et al., 2015;Gilardoni et al., 2016). Moreover, $PM_{2.5}$ may generate excess concentrations of RS in human airways, causing antioxidant depletion, oxidative stress, and respiratory diseases (Nel, 2005;Cui et al., 2015;Lakey et al., 2016;Qu et al., 2017;Lelieveld and Pöschl, 2017;Rao et al., 2018).

The formation pathways and yields of RS from ambient PM and laboratory-generated SOA have been investigated in a wide range of studies (Valavanidis et al., 2005;Ohyama et al., 2007;Chen et al., 2010;Wang et al., 2011a;Wang et al., 2011b;Verma et al., 2014;Badali et al., 2015;Bates et al., 2015;Verma et al., 2015;Arangio et al., 2016;Tong et al., 2016a;Kuang et al., 2017;Tong et al., 2017;Zhou et al., 2018;Tong et al., 2019;Chowdhury et al., 2019;Fang et al., 2019;Liu et al., 2020). The mass, surface area, and chemical composition of PM were discussed as key factors influencing the reactivity of atmospheric aerosols (Møller et al., 2010;Fang et al., 2015;Jin et al., 2019;Lammel et al., 2020). Among the substance groups associated with RS formation by PM in water are black carbon (Baumgartner et al., 2014), transition metals (Yu et al., 2018), oxidized aromatic compounds including quinones and environmentally persistent free radicals (EPFR) (Xia et al., 2004;Gehling et al., 2014;Charrier et al., 2014;Xiong et al., 2017), humic-like substances (HULIS) (Lin and Yu, 2011;Page et al., 2012;Fang et al., 2019), and peroxide-containing highly oxygenated

organic molecules (HOM) (Chen et al., 2010;Wang et al., 2011b;Tong et al., 2016a;Tong et al., 2018;Tong et al., 2019;Fang et al., 2020;Qiu et al., 2020). Moreover, the HULIS and other multifunctional compounds containing carboxyl, carboxylate, phenolic, and quinoid groups may influence the redox activity of PM via chelating transition metals (Laglera and van den Berg, 2009;Kostić et al., 2011;Catrouillet et al., 2014;Gonzalez et al., 2017;Wang et al., 2018c;Win et al., 2018;Wei et al., 2019).

To assess the oxidative potential of ambient PM, the following cellular or acellular assays have been used: dichloro-dihydro-fluorescein diacetate (DCFH-DA), dithiothreitol (DTT), ascorbic acid (AA), macrophage, electron paramagnetic resonance (EPR), and surrogate lung fluids (SLF) (Landreman et al., 2008;Charrier and Anastasio, 2012;Kalyanaraman et al., 2012;Charrier et al., 2014;Charrier and Anastasio, 2015;Fang et al., 2016;Tong et al., 2018;Bates et al., 2019;Fang et al., 2019;Molina et al., 2020;Crobeddu et al., 2020). However, the interplay of different PM constituents often results in non-additive characteristics of the RS yields or oxidative potential of PM (Charrier et al., 2014;Lakey et al., 2016;Wang et al., 2018b). Thus, unraveling the adverse health effects of ambient PM requires systematic investigations of the RS formation and chemical reactivity of PM from different sources and environments (Shiraiwa et al., 2017).

The concentration of $PM_{2.5}$ and the composition of airborne organic matter vary considerably from clean forest to polluted urban environments. For example, the $PM_{2.5}$ concentrations at the Hyytiälä forest site are typically below 10 μg m^{-3}, with organic matter accounting for ~70% (Laakso et al., 2003;Maenhaut et al., 2011), whereas the $PM_{2.5}$ concentrations in Beijing during winter can reach and exceed daily average values of 150 μg m^{-3}, with organic matter accounting for ~40% (Huang et al., 2014). Moreover, anthropogenic emissions can enhance the formation of biogenic SOA and HOM as well as the levels of particulate transition metals, humic-like substances, and PM oxidative potential (Goldstein et al., 2009;Hoyle et al., 2011;Liu et al., 2014;Xu et al., 2015;Ma et al., 2018;Pye et al., 2019;Shrivastava et al., 2019).

In this study, we compared the RS yields of $PM_{2.5}$ in clean and polluted environments. We used three approaches to explore the RS formation by $PM_{2.5}$ from remote forest of Hyytiälä (Finland), intermediately polluted city of Mainz (Germany), and heavily polluted megacity of Beijing (China) (Figure 1). To quantify

the abundances of redox-active PM constituents related to RS formation, we collected ambient $PM_{2.5}$ and measured the chemical composition of organic matter, the abundance of water-soluble transition metals, and the yield of radicals and H_2O_2 in the liquid phase (Figure 1a). To assess the influence of anthropogenic-biogenic organic matter interactions on the RS formation by ambient $PM_{2.5}$, we analyzed the radical yield of SOA generated by oxidation of mixed anthropogenic and biogenic precursors in a laboratory chamber (Figure 1b). To gain insights into the radical formation mechanism of ambient $PM_{2.5}$ in water, we differentiated the influence of transition metal ions, organic hydroperoxide (ROOH), water-soluble humic acid (HA) and fulvic acid (FA) on the radical formation by Fenton-like reactions (Figure 1c).

2 Materials and methods

2.1 Chemicals

The following chemicals were used as received without further purification: β-pinene (99%, Sigma-Aldrich), naphthalene (99.6%, Alfa Aesar GmbH&Co KG), cumene hydroperoxide (80%, Sigma-Aldrich), H_2O_2 (30%, Sigma-Aldrich), $FeSO_4 \cdot 7H_2O$ (F7002, Sigma-Aldrich), $CuSO_4 \cdot 5H_2O$ (209198, Sigma-Aldrich), $NiCl_2$ (98%, Sigma-Aldrich), $MnCl_2$ (≥ 99%, Sigma-Aldrich), VCl_2 (85%, Sigma-Aldrich), NaCl (443824T, VWR International GmbH), KH_2PO_4 (≥ 99%, Alfa Aesar GmbH&Co KG), Na_2HPO_4 (≥ 99.999%, Fluka), humic acid (53680, Sigma-Aldrich), fulvic acid (AG-CN2-0135-M005, Adipogen), 5-tert-Butoxycarbonyl-5-methyl-1-pyrroline-N-oxide (BMPO, high purity, Enzo Life Sciences, Inc.), H_2O_2 assay kit (MAK165, Sigma-Aldrich), ultra-pure water (14211-1L-F, Sigma-Aldrich), 47 mm diameter Teflon filters (JVWP04700, Omnipore membrane filter), and micropipettes (50 µL, Brand GmbH&Co KG). The used neutral saline (pH=7.4) consists of 10 mM phosphate buffer (2.2 mM KH_2PO_4 and 7.8 mM Na_2HPO_4) and 114 mM NaCl, which was used to simulate physiologically relevant condition.

2.2 Collection and extraction of ambient fine PM

Ambient fine particles were collected onto Teflon filters for all sites. The Hyytiälä $PM_{2.5}$ was collected using a three-stage cascade impactor (Dekati® PM10) at the Station for Measuring Forest Ecosystem-Atmosphere Relations station (SMEAR II station, Finland) during 31 May-19 July 2017 (Hari and Kulmala,

2005). The Mainz fine PM was collected using a micro-orifice uniform deposit impactor (MOUDI, 122-R, MSP Corporation) (Arangio et al., 2016) on the roof of the Max Planck Institute for Chemistry during 22 August-17 November 2017 and 23-31 August 2018. The Beijing winter $PM_{2.5}$ was collected using a 4-channel $PM_{2.5}$ air sampler (TH-16, Wuhan Tianhong Instruments Co., Ltd.) in the campus of the Peking University, an urban site of Beijing, during 20 December-13 January 2016 and 6 November-17 January 2018 (Lin et al., 2015). The sampling time for a single filter sample in Hyytiälä, Mainz, and Beijing are 48-72, 25-54, and 5-24 h, respectively, depending on the local PM concentrations. More information about the sampling is shown in Table S1. After sampling, all filter samples were put in petri dishes and stored in a -80 ºC freezer before analysis. To determine the mass of collected PM, each filter was weighed before and after the collection using a high sensitivity balance (±10 µg, Mettler Toledo XSE105DU). In Hyytiälä, the PM_1 and $PM_{1\text{-}2.5}$ were separately sampled, which were combined and extracted together to represent $PM_{2.5}$ samples. Mainz PM with cut-size range of 0.056-1.8 µm is taken as a proxy for $PM_{2.5}$. Particle concentrations in aqueous extracts were estimated to be in the range of 200-6000 µg mL^{-1} (Figure S1).

2.3 Formation, collection, and extraction of laboratory-generated SOA

To generate SOA from mixed anthropogenic and biogenic precursors, different concentrations of gas-phase naphthalene and β-pinene were mixed and oxidized in a potential aerosol mass (PAM) chamber, i.e., an oxidation flow reactor (OFR) (Kang et al., 2007;Tong et al., 2018). Naphthalene and β-pinene were used as representative SOA precursors in Beijing and Hyytiälä, respectively (Hakola et al., 2012;Huang et al., 2019). The concentrations of gas-phase O_3 and $^{\bullet}OH$ in the PAM chamber were ~1 ppm and ~5.0×10^{11} cm^{-3} (Tong et al., 2018), respectively. SOA was produced by adjusting the relative concentrations of naphthalene to the sum of it with β-pinene (i.e., [naphthalene]/([naphthalene] + [β-pinene])) to be ~9%, ~23%, and ~38% (mass fraction), respectively. The concentrations of naphthalene and β-pinene were 0.2-0.6 ppm and 1.0-2.5 ppm, respectively, which were determined on the basis of a calibration function measured by gas chromatography mass spectrometry (Tong et al., 2018). The number and size distributions of SOA particles were meaured using a scanning mobility particle sizer (SMPS, GRIMM Aerosol Technik

GmbH&Co. KG). When the SOA concentration was stable, 47 mm diameter Teflon filters (JVWP04700, Omnipore membrane filter) were used to collect SOA particles, which were extracted into water solutions within 2 minutes after the sampling. More information about the SOA formation, characterization, collection, and extraction can be found in previous studies (Tong et al., 2016a;Tong et al., 2017;Tong et al., 2018;Tong et al., 2019).

2.4 Surrogate mixtures

We used cumene hydroperoxide (CHP), humic acid (HA), fulvic acid (FA), and H_2O_2 as model compounds mimicking the redox-active substances in ambient particulate matter (Lin and Yu, 2011;Ma et al., 2018;Tong et al., 2019). The following method was used to prepare HA or FA solutions. First, 0-1000 μg mL^{-1} HA or FA water suspensions were made. Then, the suspensions were sonicated for 3 minutes to accelerate the dissolution of HA or FA. Afterwards, the sonicated suspensions were centrifuged at 6000 rpm (MiniStar, VWR International bvba) for 2 minutes. Finally, the supernatants were taken out from the centrifuge tubes with pipettes and stored in glass vials under 4-8 °C condition before analysis. The HA or FA solutions were prepared freshly day-to-day. To determine the concentrations of dissolved HA or FA, aliquots of the supernatants were dried with pure N_2 flow (1-2 bar) and weighted with a high sensitivity balance (± 0.01 mg, Mettler Toledo XSE105DU). The concentrations of Fe^{2+}, Cu^{2+}, HA, and H_2O_2 in the surrogate mixtures are 43 μM, 3 μM, 4 mg L^{-1}, and 7 μM, which are based on the measurement of ambient PM extracts (Fe^{2+} and Cu^{2+}, Section 2.8) or the estimated abundance in ambient PM (CHP, HA, FA, and H_2O_2, SI). To explore the influence of HA/FA on Fenton-like reactions, the radical formation in the following aqueous mixtures was also analyzed: CHP+Fe^{2+}, CHP+Cu^{2+}, CHP+Cu^{2+}+HA, CHP+Cu^{2+}+FA. The concentrations of Fe^{2+}, Cu^{2+}, HA, FA, and H_2O_2 in these solutions are 15-300 μM, 15-300 μM, 0-180 μg mL^{-1}, 0-180 μg mL^{-1}, 0-300 μM, respectively.

2.5 Quantification of radicals by EPR

5-tert-Butoxycarbonyl-5-methyl-1-pyrroline-N-oxide (BMPO) was used as a spin-trapping agent for detecting different types of radicals formed in the extracts of PM. Ambient PM or laboratory-generated

SOA were extracted from Teflon filters into 10 mM BMPO neutral saline or water solutions by vortex shaking for ~15 minutes (with Heidolph Reax 1). Around one fourth of each ambient PM filter or a whole SOA-loaded filter was used for extraction. It was assumed that most of the short-lived radicals have reacted with BMPO to form stable adducts during the extraction process.

A continuous-wave electron paramagnetic resonance (CW-EPR) X-band spectrometer (EMXplus-10/12; Bruker Corporation) was applied for the identification and quantification of radical adducts (Tong et al., 2016a;Tong et al., 2017;Tong et al., 2018;Tong et al., 2019). In order to increase the signal to noise ratio of EPR spectra, some of the extracts were concentrated by a factor of 5 - 20 through 15 - 20 minutes drying under 1-2 bar pure N_2 flow. The EPR spectra of BMPO-radical adducts were recorded by setting the following operating parameters: a microwave frequency of 9.84 GHz, a microwave power of 0.017 mW (20 dB), a receiver gain of 40 dB, a modulation amplitude of 1 G, a scan number of 50, a sweep width of 100 G, a modulation frequency of 100 kHz, a conversion time of 11 ms, and a time constant of 10 ms.

To average EPR spectra of different $PM_{2.5}$ extracts for each site, the magnetic field values of each spectrum was transformed to g-values. Then we used the Bruker software, Xenon to do the averaging, irrespective of the concentrations of $PM_{2.5}$ in extracts. The spin-counting method embedded in Xenon was applied to quantify radical adducts. The spin-counting method was calibrated using the standard compound 4-hydroxy-2,2,6,6-tetramethylpiperidin-1-oxyl (TEMPOL). To obtain the relative yields of $^{\bullet}OH$, $O_2^{\bullet-}$, C- and O-centered organic radicals, EPR spectra were simulated and fitted using the Xenon software before deconvolution (Arangio et al., 2016;Tong et al., 2018). The spin number of assigned species accounts on average for more than 95% of totally observed radical adducts, which is characterized by the peak area ratios of corresponding species. EPR spectra with low signal-to-noise ratio introduce uncertainty into the parameters describing the lineshape of peaks representing radical adducts (Tseitlin et al., 2012), causing a total quantification uncertainty of 0-19% for different types of radicals ($^{\bullet}OH$, $O_2^{\bullet-}$, C- and O-centered organic radicals etc.). The hyperfine coupling constants used for spectrum fitting are shown in Table S2.

More information on the hyperfine coupling constants of different types of BMPO radical adducts can be found in previous studies (Zhao et al., 2001;Arangio et al., 2016).

2.6 Measurement of H_2O_2 yields

We extracted ambient $PM_{2.5}$ from one fourth of each Teflon filter into 1 mL ultra-pure water or neutral saline by stirring it with a vortex shaker for ~15 minutes. Afterwards, the extracts were centrifuged at 9000 rpm (Eppendorf Minispin) for 3 minutes to remove the insoluble particles. Finally, the concentration of H_2O_2 in the supernatant was measured using the MAK165 assay kit (Yan et al., 2017;Tong et al., 2018). 50 µL of supernatant and 50 µL of a Master Mix solution containing horseradish peroxidase and Amplex Red substrate were mixed in a 96-well plate. The horseradish peroxidase catalyzed the oxidation of Amplex Red by H_2O_2 to form fluorescent resorufin (Wang et al., 2017), which was consequently quantified using a microplate reader (Synergy™ NEO, BioTek, excitation at 540 nm and emission at 590 nm) after 30 minutes of incubation. The concentration of H_2O_2 in aqueous PM extracts was determined using an H_2O_2 calibration curve based on standard H_2O_2 solutions and also corrected by blank measurements (Tong et al., 2018).

2.7 Mass spectrometry of organic compounds

By using a Q-Exactive Orbitrap mass spectrometer (Thermo Fisher Scientific, MA, USA) coupled with an ultra-high performance liquid chromatography (UHPLC) system (Dionex UltiMate 3000, Thermo Scientific, Germany) (Wang et al., 2018a;Wang et al., 2019;Tong et al., 2019), we characterized the HOM and aromatic compounds in Hyytiälä, Mainz, and Beijing winter fine PM samples in negative ionization mode. We processed the MS spectrum and UHPLC chromatogram of measured samples through a non-target screening approach by using the commercially available software SIEVE® (Thermo Fisher Scientific, MA, USA). Then, we blank-corrected the signals with peak intensity > 1×10^5. Afterwards, we used the following criteria to assign molecular formulae and filter out the irrational ones: (a) the number of atoms of C, H, O, N, S, and Cl should be in the range of 1-39, 1-72, 0-20, 0-7, 0-4, and 0-2, respectively. (b) Atomic ratios of H/C, O/C, N/C, S/C, and Cl/C should be in the range of 0.3-3, 0-3, 0-1.3, 0-0.8, and 0-0.8, respectively.

The HOM is defined as formulae in the following chemical composition range of $C_xH_yO_z$: monomers with x = 8–10, y = 12–16, z = 6–12, and z/x > 0.7; dimers with x = 17–20, y = 26–32 and z = 8–18 (Ehn et al., 2014;Tröstl et al., 2016;Tong et al., 2019). Aromatics in this study are defined to be compounds with aromaticity index (AI) > 0.5 and aromaticity equivalent (X_c) > 2.5, with the parameters accounting for the fraction of oxygen and sulfur atoms involved in π-bond structures of a compound to be set as 1 (Koch and Dittmar, 2006;Yassine et al., 2014;Tong et al., 2016b). Beyond this, the relative abundance of HOM or aromatic compounds is defined to be the sum chromatographic area of HOM or aromatics divided by the sum chromatographic area of all assigned organic compounds, with < 30% of totally detected organic compounds not assigned (Wang et al., 2018a).

2.8 Determination of water-soluble transition metal concentrations

Based on the same extraction method as the H_2O_2 analysis in section 2.6, the concentrations of five selected water-soluble transition metal species (Fe, Cu, Mn, Ni and V) in the supernatants of $PM_{2.5}$ extracts were quantified using an inductively coupled plasma mass spectrometer (ICP-MS, Agilent 7900). These five transition metal species were chosen for analysis due to their prominent concentrations and higher oxidative potential (Charrier and Anastasio, 2012). A calibration curve for the ICP-MS analysis was made by measuring standard multi-element stock solutions (Custom Grade, Inorganic Ventures). An aliquot of the supernatants was diluted and acidified using a mixture of nitric acid (5%) and hydrofluoric acid (1%), which was finalized to be 5 mL before analysis. The measured transition metal concentrations were blank-corrected and shown in corresponding figures. The detection limit of the ICP-MS analysis in this study was typically < 40 ng L^{-1}. The $PM_{2.5}$ samples collected on 2 June, 7 June, 9 June, 12 June in 2017 in Hyytiälä, on 22 August, 26 August, 28 August, 25 September, 25 October, 14 November in 2017 in Mainz, and all the 12 $PM_{2.5}$ samples from Beijing winter were used for transition metal analysis. Temporal evolution of water-soluble transition metal concentrations in water extracts of Mainz $PM_{2.5}$ were also measured, and we found that the total ion concentration of Fe, Cu, Mn, Ni, and V showed a rapid rise during the first 15 min (Figure S2a), but at a much slower rate afterwards (Figure S2b).

3 Results and discussion

3.1 Aqueous-phase radical formation from ambient $PM_{2.5}$

Figure 2a shows averaged EPR spectra of BMPO-radical adducts in neutral saline extracts of $PM_{2.5}$ samples from Hyytiälä, Mainz, and Beijing (Table S1). Each spectrum is composed of multiple peaks attributable to different types of BMPO-radical adducts. The dotted vertical lines with different colors indicate the peaks attributable to adducts of BMPO with $^{\bullet}OH$ (green), $O_2^{\bullet-}$ (orange), C- (blue) and O-centered organic radicals (purple) (Zhao et al., 2001;Arangio et al., 2016), respectively. The spectrum of Hyytiälä $PM_{2.5}$ is dominated by peaks attributable to C-centered radicals, the spectrum of Mainz $PM_{2.5}$ exhibits strong peaks attributable to C-centered radicals and $^{\bullet}OH$, and the spectrum of Beijing winter $PM_{2.5}$ is dominated by four peaks attributable to $^{\bullet}OH$.

Figure 2b shows the relative fractions (RF_{spin}) of $^{\bullet}OH$, $O_2^{\bullet-}$, C- and O-centered organic radicals averaged over multiple samples from each site. The mean RF of C- and O-centered organic radicals, respectively, were found to decrease from clean forest air samples (Hyytiälä, 66% and 11%) to polluted urban air samples (Mainz, 46% and 10%; Beijing, 39% and 5%). The high yield of C-centered radicals can be explained by rapid trapping of C-centered organic radicals ($R^{\bullet}$) by BMPO in the liquid phase (De Araujo et al., 2006). In the aqueous extracts, we applied a large excess of BMPO (10 mM of BMPO vs. ~1 µM of trapped radicals), and the estimated pseudo-first-order rate coefficient for $R^{\bullet}$ reacting with BMPO (9×10^5 s^{-1}, (Tong et al., 2018)) is much higher than the estimated $R^{\bullet}$ recombination rate coefficient (2.4×10^3, (Simic et al., 1969;Tong et al., 2018)). Moreover, rearrangement reactions in water can convert $RO^{\bullet}$ into $R^{\bullet}$ (Chevallier et al., 2004), which may warrant further investigation. The detected organic radicals are likely to comprise different molecular sizes and structures, as supported by our recent observations of organic radicals with up to 20 carbon atoms (C1-C20) formed by laboratory-generated SOA in water (Tong et al., 2018). The mean RF of $^{\bullet}OH$ was found to increase from clean forest air samples (Hyytiälä, 21%) to polluted urban air samples (Mainz 38%, Beijing 53%). The mean RF of $O_2^{\bullet-}$ varied in the range of 2-6%, showing no clear trend beyond the standard errors indicated in Figure 2b.

The formation of organic radicals, $^{\bullet}OH$, $O_2^{\bullet-}$, and H_2O_2 can be attributed to Fenton-like reactions and redox chemistry of organic and inorganic particulate matter, including environmentally persistent free radicals (EPFR), highly oxygenated organic molecules (HOM), humic-like substances (HULIS), and transition metal ions (Chevallier et al., 2004;Valavanidis et al., 2005;Li et al., 2008;Page et al., 2012;Gehling et al., 2014;Tong et al., 2016a;Tong et al., 2017;Tong et al., 2018;Tong et al., 2019;Qiu et al., 2020;Arangio et al., 2016). We speculate that hydrolytic or thermal decomposition of ROOH may play a major role in the formation of RS by $PM_{2.5}$ from remote forest locations like Hyytiälä, where large fractions of peroxide-containing HOM have been detected (Mutzel et al., 2015;Tröstl et al., 2016;Tong et al., 2019;Pye et al., 2019;Roldin et al., 2019;Bianchi et al., 2019). ROOH can generate $^{\bullet}OH$ and O-centered organic radicals through decomposition ($ROOH \rightarrow RO^{\bullet} + {}^{\bullet}OH$) and Fenton-like reactions ($Fe^{2+} + ROOH \rightarrow Fe^{3+} + RO^{\bullet} + OH^-$; $Fe^{2+} + ROOH \rightarrow Fe^{3+} + RO^- + OH^{\bullet}$) (Tong et al., 2016a). Interconversion of $RO^{\bullet}$, $R^{\bullet}$ and $ROO^{\bullet}$ radicals can lead to the formation of $O_2^{\bullet-}$ and H_2O_2 (Chevallier et al., 2004;Tong et al., 2018), which can further react with Fe^{2+} to form $^{\bullet}OH$ ($Fe^{2+} + H_2O_2 \rightarrow Fe^{3+} + {}^{\bullet}OH + OH^-$). In $PM_{2.5}$ from urban areas, transition metal ions and HULIS are expected to play a major role in aqueous-phase formation and interconversion of $^{\bullet}OH$, $O_2^{\bullet-}$ and H_2O_2 (Lloyd et al., 1997;Valavanidis et al., 2000;Zheng et al., 2013;Hayyan et al., 2016;Lakey et al., 2016;Tan et al., 2016;Kuang et al., 2017;Ma et al., 2018;Li et al., 2019).

Environmentally persistent free radicals (EPFR), are known to pre-exist in $PM_{2.5}$ at mass-specific concentration levels of ~0.2 to ~2 pmol μg^{-1}, which are an order of magnitude higher than the typical mass-specific aqueous-phase radical yields of ~0.02 to ~0.2 pmol μg^{-1} (Arangio et al., 2016;Vejerano et al., 2018;Tong et al., 2019;Chen et al., 2020). While some EPFR may be water-insoluble (Chen et al., 2018), others may directly contribute to the C-centered and O-centered radicals trapped by BMPO or participate in redox reactions yielding $^{\bullet}OH$ and $O_2^{\bullet-}$ radicals (Khachatryan et al., 2011;Arangio et al., 2016). The latter have such short chemical lifetimes that they have to be formed upon dissolution of the investigated samples immediately prior to trapping by BMPO.

The experiments and data presented in this study provide exploratory perspectives of the pathways of formation and interconversion of reactive species formed by $PM_{2.5}$ in the aqueous-phase, including highly reactive radicals and less reactive reservoir species like H_2O_2 as discussed below. A quantitative assessment, mechanistic elucidation, and full understanding will require comprehensive further experimental investigations and model calculations.

3.2 Yields of aqueous-phase radicals and H_2O_2 from ambient $PM_{2.5}$

Figure 3 shows the average air volume-specific yields and $PM_{2.5}$ mass-specific yields of aqueous-phase reactive species (RS), including radicals and H_2O_2, plotted against the $PM_{2.5}$ mass concentrations observed during the sampling periods in Hyytiälä, Mainz, and Beijing, respectively. The volume-specific yields refer to the sampled air volume and are given in units of pmol m^{-3}. They represent the absolute amounts of RS that are formed when the particulate matter is deposited in an aqueous phase such as cloud water or epithelial lining fluid, where they can contribute to atmospheric multiphase chemistry, oxidative stress and adverse health effect of PM respectively (Lakey et al., 2016;Tong et al., 2018). The mass-specific yields are normalized by the sampled mass of $PM_{2.5}$ and given in units of pmol μg^{-1}. They represent the relative amounts of aqueous RS formed per mass unit $PM_{2.5}$, enabling a direct comparison of the relative reactivity and aqueous RS-forming potential of the fine particulate matter from different sampling sites.

As illustrated in Figure 3a, the $PM_{2.5}$ concentration increased by more than an order of magnitude between the samples from Hyytiälä and Beijing (from ~5 to ~200 µg m^{-3}), and the volume-specific yield of aqueous-phase H_2O_2 exhibited a similarly strong increase (from ~10 to ~200 µg m^{-3}), while the volume-specific yield of aqueous-phase radicals exhibited a much smaller increase (from ~3 to ~7 pmol m^{-3}; Tables S1, S4, and S5). The strong increase of H_2O_2 with increasing $PM_{2.5}$ concentration is consistent with earlier studies identifying a wide range of redox-active organic and inorganic aerosol components that can produce H_2O_2 in the aqueous phase (Gunz and Hoffmann, 1990;Anastasio et al., 1994;Zuo and Deng, 1997;Arellanes et al., 2006;Chung et al., 2006;Hua et al., 2008;Möller, 2009;Wang et al., 2010;Wang et al., 2012;Anglada et al., 2015;Herrmann et al., 2015;Lakey et al., 2016;Tong et al., 2018;Bianco et al., 2020).

As illustrated in Figure 3b, the average mass-specific yields of aqueous-phase H_2O_2 were similar for the investigated urban and forest $PM_{2.5}$ samples (around 2-4 pmol μg^{-1}). In contrast, the mass-specific yield of aqueous-phase radicals was highest for the forest samples (~0.6 pmol μg^{-1}) and decreased steeply with increasing $PM_{2.5}$ mass concentration for the urban samples (~0.3 pmol μg^{-1} for Mainz, ~0.06 pmol μg^{-1} for Beijing). Accordingly, the relative fraction of radicals compared to H_2O_2 formed and detected in the aqueous phase decreased from 22% for the $PM_{2.5}$ samples from Hyytiälä to 8% for Mainz and 3% for Beijing. In other words, the aqueous H_2O_2-forming potential per mass unit of $PM_{2.5}$ was roughly the same for all investigated samples, whereas the aqueous radical-forming potential varied widely between the different samples.

The observed negative correlation with $PM_{2.5}$ mass concentration suggests that the mass-specific yield of aqueous-phase radicals from fine particulate matter may be influenced by the sample load and level of concentration in aqueous extracts, e.g., through enhanced re-combination of radicals at elevated concentration. Experiments performed at different dilutions, i.e., with varying aqueous extract volumes and concentration levels, however, suggest that observed differences in radical forming potential were not just due to different sample loads but influence by differences in the chemical composition and reactivity of the investigated $PM_{2.5}$ samples (Figure S1d and S1e). For example, the particularly high mass-specific yields of total radicals and C-centered radicals in the aqueous phase appears associated with particularly high mass fractions of organic matter in $PM_{2.5}$ from Hyytiälä (~70%, (Jimenez et al., 2009;Maenhaut et al., 2011)).

Figure 4 shows how the relative fractions (RF_{spin}) of C-centered radicals and $^{\bullet}OH$ in the aqueous phase varied with the abundance of HOM, aromatic compounds, and water-soluble transition metal ions in the investigated $PM_{2.5}$ samples (Hyytiälä and Mainz) or $PM_{2.5}$ collected at different times (Beijing). As illustrated in Figure 4a, C-centered radicals exhibited a pronounced increase with increasing HOM; whereas $^{\bullet}OH$ radicals showed a near-linear decrease. The observed increase of C-centered radicals with HOM is consistent with earlier studies indicating that peroxide-containing HOM may play an important role in organic radical formation (Tong et al., 2016a;Tong et al., 2019). In contrast, the C-centered radicals did not

exhibit an increase but a decrease with increasing abundance of aromatic compounds (Figure 4b). This is consistent with ability of certain aromatic compounds like quinones and semiquinones to enhance redox cycling and the formation of •OH radicals in analogy to Fenton reactions (Chung et al., 2006;Zhang and Tao, 2009;Khachatryan et al., 2011;Elser et al., 2016;Fan et al., 2016;Lakey et al., 2016;An et al., 2019). As illustrated in Figure 4c, C-centered radicals exhibited a pronounced decrease with transition metal ions, whereas •OH radicals exhibited a near-linear increase. These findings are consistent with the role of transition metal ions in Fenton-like reactions efficiently converting H_2O_2 and hydroperoxides into •OH radicals, and with studies reporting that metal-organic interactions may alter the oxidative potential particulate matter under atmospheric and physiological conditions (Zuo and Hoigne, 1992;Lakey et al., 2016;Singh and Gupta, 2016;Cheng et al., 2017;Wang et al., 2018b;Wei et al., 2019;Lin and Yu, 2020). To gain further insights into the complex interactions of organic particulate matter, transition metal ions, and reactive species in the aqueous phase, we performed experiments with laboratory-generated secondary organic aerosols and surrogate mixtures of atmospherically relevant substance classes as detailed in the following sections.

3.3 Aqueous-phase radical yields of laboratory-generated SOA

To investigate the influence of biogenic and anthropogenic secondary organic aerosols (SOA) on aqueous-phase radical formation, we performed experiments with SOA from naphthalene and β-pinene oxidized by O_3 and •OH in a PAM chamber (Sect. 2.3).

As illustrated in Figure 5a, we found a steep non-linear increase of the mass-specific radical yield with increasing precursor mass fraction of β-pinene from ~2 pmol μg^{-1} for pure naphthalene SOA to ~8 pmol μg^{-1} for pure β-pinene SOA, which is consistent with related earlier investigations that found higher radical yields for biogenic SOA compared to anthropogenic SOA (Tong et al., 2016a;Tong et al., 2017;Tong et al., 2018;Tong et al., 2019).

Figure 5b shows that β-pinene SOA mainly generates •OH (~86%), whereas naphthalene SOA and mixtures of naphthalene and β-pinene SOA mainly generate $O_2^{\bullet-}$ (60-77%) and C-centered radicals (18-

34%). Substantial formation of $O_2^{\bullet-}$ by terpene SOA is consistent with a recent study, showing that $O_2^{\bullet-}$ formation via $^{\bullet}OH$ oxidation of primary or secondary alcohols followed by unimolecular decomposition of α-hydroxyperoxyl radicals (Wei et al., 2021). The small RF of $^{\bullet}OH$ generated by naphthalene SOA may appear in contrast to the high RF of $^{\bullet}OH$ generated $PM_{2.5}$ from Beijing that contains substantial amounts of aromatics (Figure 4b). Note, however, that the composition of $PM_{2.5}$ from Beijing is much more complex than that of laboratory-generated naphthalene SOA. For example, Fenton-like reactions of transition metal ions are expected to generate $^{\bullet}OH$ in ambient $PM_{2.5}$ (Kehrer, 2000;Tong et al., 2016a), whereas the laboratory-generated SOA does not contain significant amounts of transition metals.

3.4 Aqueous-phase radical yields of surrogate mixtures

To investigate the influence of different types of redox-active components in $PM_{2.5}$ on the total yield of radicals in the aqueous phase and on the relative fractions (RF_{spin}) of different types of radicals, we performed experiments with aqueous surrogate mixtures of Fe^{2+}, Cu^{2+}, humic acid (HA), fulvic acid (FA), cumene hydroperoxide (CHP), and H_2O_2 in varying concentrations. Figure 6 shows that increasing concentrations of organic hydroperoxide (here CHP) can lead to a near-linear increase of total radical concentration in the aqueous phase (Figure 6a), and to a strong increase of RF_{spin} for C-centered radicals (Figure 6b). The increase of $R^{\bullet}$ with CHP is consistent with the high RF_{spin} for C-centered radicals in $PM_{2.5}$ from Hyytiälä (Figure 2b), which contains a large fraction of HOM (Tong et al., 2019). Increasing concentrations of H_2O_2 also led to a near-linear increase of increase of total radical concentration in the aqueous phase (Figure 6c) as well as a strong increase of $^{\bullet}OH$ (Figure 6d). The strong increase of aqueous-phase $^{\bullet}OH$ with H_2O_2 indicates that gas-particle partitioning and multiphase chemical reactions of gas-phase oxidants can substantially influence the generation of radicals and oxidative stress by ambient $PM_{2.5}$.

For increasing concentrations of humic acid (HA), we observed a strong non-linear decrease of total radical concentration in the aqueous phase (Figure 6e), and to a strong increase of RF_{spin} for C-centered radicals (Figure 6f). The decreasing radical concentration is likely due to the ability of HA to bind/chelate iron and other metal ions (Graber and Rudich, 2006;Laglera and van den Berg, 2009;Scheinhardt et al.,

2013;Tang et al., 2014;Yang et al., 2017), which may lead to a suppression of radical formation via Fenton-like reactions. Moreover, humic substances can act as antioxidants and radical scavengers (Aeschbacher et al., 2012). The fractional increase of C-centered radicals reflects the involvement of HA in complex radical chemistry (Shi et al., 2020). Compared to HA, the effects of fulvic acid (FA) were qualitatively similar but quantitatively less pronounced (Figures. 6g and 6h), which is consistent with earlier studies investigating the metal ion binding capacity and redox chemistry of FA (Wang et al., 1996;Graber and Rudich, 2006;Scheinhardt et al., 2013;Tang et al., 2014;Gonzalez et al., 2017;Yang et al., 2017). Different reactivities of HA and FA are also reflected by the different RF values of $O_2^{\bullet-}$ and C-centered radicals observed at high concentrations of FA and HA (Figure 6h vs. Figure 6f) as well as in reactions mixtures with copper instead of iron ions (Figure S6). Further investigations will be required to resolve the underlying reaction mechanisms and kinetics.

4 Conclusions and implications

In this study, we investigated the formation of aqueous-phase H_2O_2 and radicals by aerosol samples from remote forest and polluted urban air. The aqueous H_2O_2-forming potential per mass unit of $PM_{2.5}$ was roughly the same for all investigated samples, whereas the mass-specific yields of radicals were lower for sampling sites with higher concentration of ambient $PM_{2.5}$.

The abundances of water-soluble transition metals in ambient $PM_{2.5}$ were positively correlated with the relative fraction of $^{\bullet}OH$ and negatively correlated with the relative fraction of carbon-centered radicals, which can be attributed to Fenton-like reactions. In contrast, HOM was negatively correlated with the relative fraction of $^{\bullet}OH$ and positively correlated with the relative fraction of carbon-centered radicals, which is consistent with related earlier studies indicating that peroxide-containing HOM may play an important role in organic radical formation (Tong et al., 2016a;Tong et al., 2019).

We found that the relative fractions of different types of radicals formed by ambient $PM_{2.5}$ were comparable to surrogate mixtures comprising transition metal ions, organic hydroperoxide, H_2O_2, and humic or fulvic acids. Our results show that the interplay of transition metal ions (e.g., iron and copper

ions), highly oxidized organic molecules (e.g., hydroperoxides), and complexing or scavenging agents (e.g., humic or fulvic acids) leads to non-linear concentration dependencies in the aqueous-phase RS production. A strong dependence on chemical composition was also observed for the aqueous-phase radical yields of laboratory-generated SOA from precursor mixtures of naphthalene and β-pinene.

Overall, our findings show how the composition of $PM_{2.5}$ can influence the amount and nature of aqueous-phase RS, which may explain differences in the chemical reactivity and health effects of particulate matter in clean and polluted air. Further investigations will be required to resolve the influence of biogenic and anthropogenic pollutants on atmospheric chemistry, air quality, and public health in the Anthropocene (Pöschl and Shiraiwa, 2015;Cheng et al., 2016;Shiraiwa et al., 2017;An et al., 2019;Roldin et al., 2019;Daellenbach et al., 2020;Fang et al., 2020;Lelieveld et al., 2020;Lin and Yu, 2020;Pöschl, 2020;Su et al., 2020;Tao et al., 2020;Yun et al., 2020;Zheng et al., 2020;Wang et al., 2021).

References

Aeschbacher, M., Graf, C., Schwarzenbach, R. P., and Sander, M.: Antioxidant properties of humic substances, Environ. Sci. Technol., 46, 4916-4925, 2012.

An, Z., Huang, R.-J., Zhang, R., Tie, X., Li, G., Cao, J., Zhou, W., Shi, Z., Han, Y., and Gu, Z.: Severe haze in Northern China: A synergy of anthropogenic emissions and atmospheric processes, Proc. Natl. Acad. Sci. U.S.A., 116, 8657-8666, 2019.

Anastasio, C., Faust, B. C., and Allen, J. M.: Aqueous phase photochemical formation of hydrogen peroxide in authentic cloud waters, J. Geophys. Res. Atmos., 99, 8231-8248, 1994.

Anglada, J. M., Martins-Costa, M., Francisco, J. S., and Ruiz-Lopez, M. F.: Interconnection of reactive oxygen species chemistry across the interfaces of atmospheric, environmental, and biological processes, Acc. Chem. Res., 48, 575-583, 2015.

Arangio, A. M., Tong, H., Socorro, J., Pöschl, U., and Shiraiwa, M.: Quantification of environmentally persistent free radicals and reactive oxygen species in atmospheric aerosol particles, Atmos. Chem. Phys., 16, 13105-13119, 2016.

Arellanes, C., Paulson, S. E., Fine, P. M., and Sioutas, C.: Exceeding of Henry's law by hydrogen peroxide associated with urban aerosols, Environ. Sci. Technol., 40, 4859-4866, 2006.

Badali, K., Zhou, S., Aljawhary, D., Antiñolo, M., Chen, W., Lok, A., Mungall, E., Wong, J., Zhao, R., and Abbatt, J.: Formation of hydroxyl radicals from photolysis of secondary organic aerosol material, Atmos. Chem. Phys., 15, 7831-7840, 2015.

Bates, J. T., Weber, R. J., Abrams, J., Verma, V., Fang, T., Klein, M., Strickland, M. J., Sarnat, S. E., Chang, H. H., and Mulholland, J. A.: Reactive oxygen species generation linked to sources of atmospheric particulate matter and cardiorespiratory effects, Environ. Sci. Technol., 49, 13605-13612, 2015.

Bates, J. T., Fang, T., Verma, V., Zeng, L., Weber, R. J., Tolbert, P. E., Abrams, J. Y., Sarnat, S. E., Klein, M., Mulholland, J. A., and Russell, A. G.: Review of acellular assays of ambient particulate matter oxidative potential: Methods and relationships with composition, sources, and health effects, Environ. Sci. Technol., 53, 4003-4019, 2019.

Baumgartner, J., Zhang, Y., Schauer, J. J., Huang, W., Wang, Y., and Ezzati, M.: Highway proximity and black carbon from cookstoves as a risk factor for higher blood pressure in rural China, Proc. Natl. Acad. Sci. U.S.A., 111, 13229-13234, 2014.

Bianchi, F., Kurtén, T., Riva, M., Mohr, C., Rissanen, M. P., Roldin, P., Berndt, T., Crounse, J. D., Wennberg, P. O., and Mentel, T. F.: Highly oxygenated organic molecules (HOM) from gas-phase autoxidation involving peroxy radicals: A key contributor to atmospheric aerosol, Chem. Rev., 119, 3472-3509, 2019.

Bianco, A., Passananti, M., Brigante, M., and Mailhot, G.: Photochemistry of the Cloud Aqueous Phase: A Review, Molecules, 25, 423, 2020.

Catrouillet, C., Davranche, M., Dia, A., Bouhnik-Le Coz, M., Marsac, R., Pourret, O., and Gruau, G.: Geochemical modeling of Fe (II) binding to humic and fulvic acids, Chem. Geol., 372, 109-118, 2014.

Charrier, J., and Anastasio, C.: On dithiothreitol (DTT) as a measure of oxidative potential for ambient particles: evidence for the importance of soluble transition metals, Atmos. Chem. Phys., 12, 9321-9333, 2012.

Charrier, J. G., McFall, A. S., Richards-Henderson, N. K., and Anastasio, C.: Hydrogen peroxide formation in a surrogate lung fluid by transition metals and quinones present in particulate matter, Environ. Sci. Technol., 48, 7010-7017, 2014.

Charrier, J. G., and Anastasio, C.: Rates of hydroxyl radical production from transition metals and quinones in a surrogate lung fluid, Environ. Sci. Technol., 49, 9317-9325, 2015.

Chen, Q., Sun, H., Wang, M., Mu, Z., Wang, Y., Li, Y., Wang, Y., Zhang, L., and Zhang, Z.: Dominant fraction of EPFRs from nonsolvent-extractable organic matter in fine particulates over Xi'an, China, Environ. Sci. Technol., 52, 9646-9655, 2018.

Chen, Q., Sun, H., Song, W., Cao, F., Tian, C., and Zhang, Y.-L.: Size-resolved exposure risk of persistent free radicals (PFRs) in atmospheric aerosols and their potential sources, Atmos. Chem. Phys., 20, 14407-14417, 2020.

Chen, X., Hopke, P. K., and Carter, W. P.: Secondary organic aerosol from ozonolysis of biogenic volatile organic compounds: chamber studies of particle and reactive oxygen species formation, Environ. Sci. Technol., 45, 276-282, 2010.

Cheng, C., Li, M., Chan, C. K., Tong, H., Chen, C., Chen, D., Wu, D., Li, L., Wu, C., and Cheng, P.: Mixing state of oxalic acid containing particles in the rural area of Pearl River Delta, China: implications for the formation mechanism of oxalic acid, Atmos. Chem. Phys., 17, 9519-9533, 2017.

Cheng, Y., Zheng, G., Wei, C., Mu, Q., Zheng, B., Wang, Z., Gao, M., Zhang, Q., He, K., and Carmichael, G.: Reactive nitrogen chemistry in aerosol water as a source of sulfate during haze events in China, Sci. Adv., 2, e1601530, 2016.

Chevallier, E., Jolibois, R. D., Meunier, N., Carlier, P., and Monod, A.: "Fenton-like" reactions of methylhydroperoxide and ethylhydroperoxide with Fe^{2+} in liquid aerosols under tropospheric conditions, Atmos. Environ., 38, 921-933, 2004.

Chowdhury, P. H., He, Q., Carmieli, R., Li, C., Rudich, Y., and Pardo, M.: Connecting the Oxidative Potential of Secondary Organic Aerosols with Reactive Oxygen Species in Exposed Lung Cells, Environ. Sci. Technol., 53, 13949-13958, 2019.

Chung, M. Y., Lazaro, R. A., Lim, D., Jackson, J., Lyon, J., Rendulic, D., and Hasson, A. S.: Aerosol-borne quinones and reactive oxygen species generation by particulate matter extracts, Environ. Sci. Technol., 40, 4880-4886, 2006.

Crobeddu, B., Baudrimont, I., Deweirdt, J., Sciare, J., Badel, A., Camproux, A.-C., Bui, L. C., and Baeza-Squiban, A.: Lung Antioxidant Depletion: A Predictive Indicator of Cellular Stress Induced by Ambient Fine Particles, Environ. Sci. Technol., 54, 2360-2369, 2020.

Cui, Y., Xie, X., Jia, F., He, J., Li, Z., Fu, M., Hao, H., Liu, Y., Liu, J. Z., and Cowan, P. J.: Ambient fine particulate matter induces apoptosis of endothelial progenitor cells through reactive oxygen species formation, Cell Physiol. Biochem., 35, 353-363, 2015.

Daellenbach, K. R., Uzu, G., Jiang, J., Cassagnes, L.-E., Leni, Z., Vlachou, A., Stefenelli, G., Canonaco, F., Weber, S., and Segers, A.: Sources of particulate-matter air pollution and its oxidative potential in Europe, Nature, 587, 414-419, 2020.

De Araujo, M., De M. Carneiro, J., and Taranto, A.: Solvent effects on the relative stability of radicals derived from artemisinin: DFT study using the PCM/COSMO approach, Int. J. Quantum. Chem., 106, 2804-2810, 2006.

Donaldson, D., and Valsaraj, K. T.: Adsorption and reaction of trace gas-phase organic compounds on atmospheric water film surfaces: A critical review, Environ. Sci. Technol., 44, 865-873, 2010.

Ehn, M., Thornton, J. A., Kleist, E., Sipilä, M., Junninen, H., Pullinen, I., Springer, M., Rubach, F., Tillmann, R., and Lee, B.: A large source of low-volatility secondary organic aerosol, Nature, 506, 476-479, 2014.

Elser, M., Huang, R.-J., Wolf, R., Slowik, J. G., Wang, Q., Canonaco, F., Li, G., Bozzetti, C., Daellenbach, K. R., and Huang, Y.: New insights into $PM_{2.5}$ chemical composition and sources in two major cities in China during extreme haze events using aerosol mass spectrometry, Atmos. Chem. Phys., 16, 3207-3225, 2016.

Enami, S., Sakamoto, Y., and Colussi, A. J.: Fenton chemistry at aqueous interfaces, Proc. Natl. Acad. Sci. U.S.A., 111, 623-628, 2014.

Ervens, B., Turpin, B., and Weber, R.: Secondary organic aerosol formation in cloud droplets and aqueous particles (aqSOA): a review of laboratory, field and model studies, Atmos. Chem. Phys., 11, 11069-11102, 2011.

Fan, X., Wei, S., Zhu, M., Song, J., and Peng, P. a.: Comprehensive characterization of humic-like substances in smoke $PM_{2.5}$ emitted from the combustion of biomass materials and fossil fuels, Atmos. Chem. Phys., 16, 13321-13340, 2016.

Fang, T., Guo, H., Verma, V., Peltier, R., and Weber, R.: $PM_{2.5}$ water-soluble elements in the southeastern United States: automated analytical method development, spatiotemporal distributions, source apportionment, and implications for heath studies, Atmos. Chem. Phys., 15, 11667-11682, 2015.

Fang, T., Verma, V., Bates, J. T., Abrams, J., Klein, M., Strickland, M. J., Sarnat, S. E., Chang, H. H., Mulholland, J. A., and Tolbert, P. E.: Oxidative potential of ambient water-soluble $PM_{2.5}$ in the southeastern United States: contrasts in sources and health associations between ascorbic acid (AA) and dithiothreitol (DTT) assays, Atmos. Chem. Phys., 16, 3865-3879, 2016.

Fang, T., Lakey, P. S. J., Weber, R. J., and Shiraiwa, M.: Oxidative Potential of Particulate Matter and Generation of Reactive Oxygen Species in Epithelial Lining Fluid, Environ. Sci. Technol., 53, 12784-12792, 2019.

Fang, T., Lakey, P. S. J., Rivera-Rios, J. C., Keutsch, F. N., and Shiraiwa, M.: Aqueous-Phase Decomposition of Isoprene Hydroxy Hydroperoxide and Hydroxyl Radical Formation by Fenton-Like Reactions with Iron Ions, J. Phys. Chem. A, 124, 5230-5236, 2020.

Gehling, W., Khachatryan, L., and Dellinger, B.: Hydroxyl radical generation from environmentally persistent free radicals (EPFRs) in $PM_{2.5}$, Environ. Sci. Technol., 48, 4266-4272, 2014.

Gilardoni, S., Massoli, P., Paglione, M., Giulianelli, L., Carbone, C., Rinaldi, M., Decesari, S., Sandrini, S., Costabile, F., and Gobbi, G. P.: Direct observation of aqueous secondary organic aerosol from biomass-burning emissions, Proc. Natl. Acad. Sci. U.S.A., 113, 10013-10018, 2016.

Gligorovski, S., Strekowski, R., Barbati, S., and Vione, D.: Environmental implications of hydroxyl radicals ($^{\bullet}OH$), Chem. Rev., 115, 13051-13092, 2015.

Goldstein, A. H., Koven, C. D., Heald, C. L., and Fung, I. Y.: Biogenic carbon and anthropogenic pollutants combine to form a cooling haze over the southeastern United States, Proc. Natl. Acad. Sci. U.S.A., 106, 8835-8840, 2009.

Gonzalez, D. H., Cala, C. K., Peng, Q., and Paulson, S. E.: HULIS enhancement of hydroxyl radical formation from Fe(II): Kinetics of fulvic acid–Fe(II) complexes in the presence of lung antioxidants, Environ. Sci. Technol., 51, 7676-7685, 2017.

Graber, E., and Rudich, Y.: Atmospheric HULIS: How humic-like are they? A comprehensive and critical review, Atmos. Chem. Phys., 6, 729-753, 2006.

Gunz, D. W., and Hoffmann, M. R.: Atmospheric chemistry of peroxides: a review, Atmos. Environ., 24, 1601-1633, 1990.

Hakola, H., Hellén, H., Hemmilä, M., Rinne, J., and Kulmala, M.: In situ measurements of volatile organic compounds in a boreal forest, Atmos. Chem. Phys., 12, 11665-11678, 2012.

Halliwell, B., and Whiteman, M.: Measuring reactive species and oxidative damage in vivo and in cell culture: how should you do it and what do the results mean?, Br. J. Pharmacol., 142, 231-255, 2004.

570 Hari, P., and Kulmala, M.: Station for Measuring EcosystemsAtmosphere Relations (SMEAR II), Boreal
571 Env. Res., 10, 315-322, 2005.
572 Hayyan, M., Hashim, M. A., and AlNashef, I. M.: Superoxide ion: generation and chemical implications,
573 Chem. Rev., 116, 3029-3085, 2016.
574 Herrmann, H., Schaefer, T., Tilgner, A., Styler, S. A., Weller, C., Teich, M., and Otto, T.: Tropospheric
575 aqueous-phase chemistry: kinetics, mechanisms, and its coupling to a changing gas phase, Chem. Rev., 115,
576 4259-4334, 2015.
577 Hoyle, C. R., Boy, M., Donahue, N. M., Fry, J. L., Glasius, M., Guenther, A., Hallar, A. G., Huff Hartz, K.,
578 Petters, M. D., and Petäjä, T.: A review of the anthropogenic influence on biogenic secondary organic
579 aerosol, Atmos. Chem. Phys., 11, 321-343, 2011.
580 Hua, W., Chen, Z., Jie, C., Kondo, Y., Hofzumahaus, A., Takegawa, N., Chang, C., Lu, K., Miyazaki, Y.,
581 and Kita, K.: Atmospheric hydrogen peroxide and organic hydroperoxides during PRIDE-PRD'06, China:
582 their concentration, formation mechanism and contribution to secondary aerosols, Atmos. Chem. Phys., 8,
583 6755-6773, 2008.
584 Huang, G., Liu, Y., Shao, M., Li, Y., Chen, Q., Zheng, Y., Wu, Z., Liu, Y., Wu, Y., Hu, M., Li, X., Lu, S.,
585 Wang, C., Liu, J., Zheng, M., and Zhu, T.: Potentially Important Contribution of Gas-Phase Oxidation of
586 Naphthalene and Methylnaphthalene to Secondary Organic Aerosol during Haze Events in Beijing, Environ.
587 Sci. Technol., 53, 1235-1244, 2019.
588 Huang, R.-J., Zhang, Y., Bozzetti, C., Ho, K.-F., Cao, J.-J., Han, Y., Daellenbach, K. R., Slowik, J. G., Platt,
589 S. M., and Canonaco, F.: High secondary aerosol contribution to particulate pollution during haze events
590 in China, Nature, 514, 218-222, 2014.
591 Jacob, D. J.: Heterogeneous chemistry and tropospheric ozone, Atmos. Environ., 34, 2131-2159, 2000.
592 Jimenez, J. L., Canagaratna, M., Donahue, N., Prevot, A., Zhang, Q., Kroll, J. H., DeCarlo, P. F., Allan, J.
593 D., Coe, H., and Ng, N.: Evolution of organic aerosols in the atmosphere, Science, 326, 1525-1529, 2009.
594 Jin, L., Xie, J., Wong, C. K., Chan, S. K., Abbaszade, G. l., Schnelle-Kreis, J. r., Zimmermann, R., Li, J.,
595 Zhang, G., and Fu, P.: Contributions of city-specific fine particulate matter ($PM_{2.5}$) to differential in vitro
596 oxidative stress and toxicity implications between Beijing and Guangzhou of China, Environ. Sci. Technol.,
597 53, 2881-2891, 2019.
598 Kalyanaraman, B., Darley-Usmar, V., Davies, K. J., Dennery, P. A., Forman, H. J., Grisham, M. B., Mann,
599 G. E., Moore, K., Roberts II, L. J., and Ischiropoulos, H.: Measuring reactive oxygen and nitrogen species
600 with fluorescent probes: challenges and limitations, Free Radic. Biol. Med., 52, 1-6, 2012.
601 Kang, E., Root, M., Toohey, D., and Brune, W. H.: Introducing the concept of potential aerosol mass (PAM),
602 Atmos. Chem. Phys., 7, 5727-5744, 2007.
603 Kehrer, J. P.: The Haber–Weiss reaction and mechanisms of toxicity, Toxicology, 149, 43-50, 2000.

Khachatryan, L., Vejerano, E., Lomnicki, S., and Dellinger, B.: Environmentally persistent free radicals (EPFRs). 1. Generation of reactive oxygen species in aqueous solutions, Environ. Sci. Technol., 45, 8559-8566, 2011.

Koch, B., and Dittmar, T.: From mass to structure: An aromaticity index for high‐resolution mass data of natural organic matter, Rapid Commun. Mass Spectrom., 20, 926-932, 2006.

Kostić, I., Anđelković, T., Nikolić, R., Bojić, A., Purenović, M., Blagojević, S., and Anđelković, D.: Copper(II) and lead(II) complexation by humic acid and humic-like ligands, J. Serb. Chem. Soc., 76, 1325-1336, 2011.

Kuang, X. M., Scott, J. A., da Rocha, G. O., Betha, R., Price, D. J., Russell, L. M., Cocker, D. R., and Paulson, S. E.: Hydroxyl radical formation and soluble trace metal content in particulate matter from renewable diesel and ultra low sulfur diesel in at-sea operations of a research vessel, Aerosol Sci. Technol., 51, 147-158, 2017.

Laakso, L., Hussein, T., Aarnio, P., Komppula, M., Hiltunen, V., Viisanen, Y., and Kulmala, M.: Diurnal and annual characteristics of particle mass and number concentrations in urban, rural and Arctic environments in Finland, Atmos. Environ., 37, 2629-2641, 2003.

Laglera, L. M., and van den Berg, C. M.: Evidence for geochemical control of iron by humic substances in seawater, Limnol. Oceanogr., 54, 610-619, 2009.

Lakey, P. S., Berkemeier, T., Tong, H., Arangio, A. M., Lucas, K., Pöschl, U., and Shiraiwa, M.: Chemical exposure-response relationship between air pollutants and reactive oxygen species in the human respiratory tract, Sci. Rep., 6, 32916, 2016.

Lammel, G., Kitanovski, Z., Kukucka, P., Novak, J., Arangio, A. M., Codling, G. P., Filippi, A., Hovorka, J., Kuta, J., and Leoni, C.: Oxygenated and Nitrated Polycyclic Aromatic Hydrocarbons in Ambient Air—Levels, Phase Partitioning, Mass Size Distributions, and Inhalation Bioaccessibility, Environ. Sci. Technol., 54, 2615-2625, 2020.

Landreman, A. P., Shafer, M. M., Hemming, J. C., Hannigan, M. P., and Schauer, J. J.: A macrophage-based method for the assessment of the reactive oxygen species (ROS) activity of atmospheric particulate matter (PM) and application to routine (daily-24 h) aerosol monitoring studies, Aerosol Sci. Technol., 42, 946-957, 2008.

Lelieveld, J., and Pöschl, U.: Chemists can help to solve the air-pollution health crisis, Nature, 551, 291-293, 2017.

Lelieveld, J., Pozzer, A., Pöschl, U., Fnais, M., Haines, A., and Münzel, T.: Loss of life expectancy from air pollution compared to other risk factors: a worldwide perspective, Cardiovasc. Res., doi:10.1093/cvr/cvaa025, 2020.

Li, N., Xia, T., and Nel, A. E.: The role of oxidative stress in ambient particulate matter-induced lung diseases and its implications in the toxicity of engineered nanoparticles, Free Radic. Biol. Med., 44, 1689-1699, 2008.

Li, X., Kuang, X. M., Yan, C., Ma, S., Paulson, S. E., Zhu, T., Zhang, Y., and Zheng, M.: Oxidative potential by $PM_{2.5}$ in the North China Plain: generation of hydroxyl radical, Environ. Sci. Technol., 53, 512-520, 2018.

Li, X., Han, J., Hopke, P. K., Hu, J., Shu, Q., Chang, Q., and Ying, Q.: Quantifying primary and secondary humic-like substances in urban aerosol based on emission source characterization and a source-oriented air quality model, Atmos. Chem. Phys., 19, 2327-2341, 2019.

Lin, M., and Yu, J. Z.: Assessment of interactions between transition metals and atmospheric organics: Ascorbic Acid Depletion and Hydroxyl Radical Formation in Organic-metal Mixtures, Environ. Sci. Technol., 54, 1431−1442, 2020.

Lin, P., and Yu, J. Z.: Generation of reactive oxygen species mediated by humic-like substances in atmospheric aerosols, Environ. Sci. Technol., 45, 10362-10368, 2011.

Lin, Y., Ma, Y., Qiu, X., Li, R., Fang, Y., Wang, J., Zhu, Y., and Hu, D.: Sources, transformation, and health implications of PAHs and their nitrated, hydroxylated, and oxygenated derivatives in $PM_{2.5}$ in Beijing, J. Geophys. Res. Atmos., 120, 7219-7228, 2015.

Liu, F., Saavedra, M. G., Champion, J. A., Griendling, K. K., and Ng, N. L.: Prominent Contribution of Hydrogen Peroxide to Intracellular Reactive Oxygen Species Generated upon Exposure to Naphthalene Secondary Organic Aerosols, Environ. Sci. Technol. Lett., 7, 171-177, 2020.

Liu, Q., Baumgartner, J., Zhang, Y., Liu, Y., Sun, Y., and Zhang, M.: Oxidative potential and inflammatory impacts of source apportioned ambient air pollution in Beijing, Environ. Sci. Technol., 48, 12920-12929, 2014.

Lloyd, R. V., Hanna, P. M., and Mason, R. P.: The origin of the hydroxyl radical oxygen in the Fenton reaction, Free Radical Biol. Med., 22, 885-888, 1997.

Ma, Y., Cheng, Y., Qiu, X., Cao, G., Fang, Y., Wang, J., Zhu, T., Yu, J., and Hu, D.: Sources and oxidative potential of water-soluble humic-like substances (HULIS WS) in fine particulate matter ($PM_{2.5}$) in Beijing, Atmos. Chem. Phys., 18, 5607-5617, 2018.

Maenhaut, W., Nava, S., Lucarelli, F., Wang, W., Chi, X., and Kulmala, M.: Chemical composition, impact from biomass burning, and mass closure for $PM_{2.5}$ and PM_{10} aerosols at Hyytiälä, Finland, in summer 2007, X-Ray Spectrom., 40, 168-171, 2011.

Molina, C., Toro, R., Manzano, C., Canepari, S., Massimi, L., and Leiva-Guzmán, M. A.: Airborne aerosols and human health: Leapfrogging from mass concentration to oxidative potential, Atmosphere, 11, 917, 2020.

Möller, D.: Atmospheric hydrogen peroxide: Evidence for aqueous-phase formation from a historic perspective and a one-year measurement campaign, Atmos. Environ., 43, 5923-5936, 2009.

Møller, P., Jacobsen, N. R., Folkmann, J. K., Danielsen, P. H., Mikkelsen, L., Hemmingsen, J. G., Vesterdal, L. K., Forchhammer, L., Wallin, H., and Loft, S.: Role of oxidative damage in toxicity of particulates, Free Radic. Res., 44, 1-46, 2010.

Mutzel, A., Poulain, L., Berndt, T., Iinuma, Y., Rodigast, M., Böge, O., Richters, S., Spindler, G., Sipilä, M., Jokinen, T., Markku, K., and Hartmut, H.: Highly oxidized multifunctional organic compounds observed in tropospheric particles: A field and laboratory study, Environ. Sci. Technol., 49, 7754-7761, 2015.

Nel, A.: Air pollution-related illness: effects of particles, Science, 308, 804-806, 2005.

Ohyama, M., Otake, T., Adachi, S., Kobayashi, T., and Morinaga, K.: A comparison of the production of reactive oxygen species by suspended particulate matter and diesel exhaust particles with macrophages, Inhal. Toxicol., 19, 157-160, 2007.

Page, S. E., Sander, M., Arnold, W. A., and McNeill, K.: Hydroxyl radical formation upon oxidation of reduced humic acids by oxygen in the dark, Environ. Sci. Technol., 46, 1590-1597, 2012.

Park, J., Park, E. H., Schauer, J. J., Yi, S.-M., and Heo, J.: Reactive oxygen species (ROS) activity of ambient fine particles ($PM_{2.5}$) measured in Seoul, Korea, Environ. Int., 117, 276-283, 2018.

Pöschl, U.: Air Pollution, Oxidative Stress, and Public Health in the Anthropocene, in: Health of People, Health of Planet and Our Responsibility, Springer, Cham, 79-92, 2020.

Pöschl, U., and Shiraiwa, M.: Multiphase chemistry at the atmosphere–biosphere interface influencing climate and public health in the anthropocene, Chem. Rev., 115, 4440-4475, 2015.

Pye, H. O., D'Ambro, E. L., Lee, B. H., Schobesberger, S., Takeuchi, M., Zhao, Y., Lopez-Hilfiker, F., Liu, J., Shilling, J. E., and Xing, J.: Anthropogenic enhancements to production of highly oxygenated molecules from autoxidation, Proc. Natl. Acad. Sci. U.S.A., 116, 6641-6646, 2019.

Qiu, J., Liang, Z., Tonokura, K., Colussi, A. J., and Enami, S.: Stability of Monoterpene-Derived α-Hydroxyalkyl-Hydroperoxides in Aqueous Organic Media: Relevance to the Fate of Hydroperoxides in Aerosol Particle Phases, Environ. Sci. Technol., 54, 3890-3899, 2020.

Qu, J., Li, Y., Zhong, W., Gao, P., and Hu, C.: Recent developments in the role of reactive oxygen species in allergic asthma, J. Thorac. Dis., 9, E32, 2017.

Rao, X., Zhong, J., Brook, R. D., and Rajagopalan, S.: Effect of particulate matter air pollution on cardiovascular oxidative stress pathways, Antioxid. Redox. Signal., 28, 797-818, 2018.

Reinmuth-Selzle, K., Kampf, C. J., Lucas, K., Lang-Yona, N., Fröhlich-Nowoisky, J., Shiraiwa, M., Lakey, P. S., Lai, S., Liu, F., and Kunert, A. T.: Air pollution and climate change effects on allergies in the

anthropocene: abundance, interaction, and modification of allergens and adjuvants, Environ. Sci. Technol., 51, 4119-4141, 2017.

Roldin, P., Ehn, M., Kurtén, T., Olenius, T., Rissanen, M. P., Sarnela, N., Elm, J., Rantala, P., Hao, L., and Hyttinen, N.: The role of highly oxygenated organic molecules in the Boreal aerosol-cloud-climate system, Nat. Commun., 10, 1-15, 2019.

Scheinhardt, S., Müller, K., Spindler, G., and Herrmann, H.: Complexation of trace metals in size-segregated aerosol particles at nine sites in Germany, Atmos. Environ., 74, 102-109, 2013.

Shi, Y., Dai, Y., Liu, Z., Nie, X., Zhao, S., Zhang, C., and Jia, H.: Light-induced variation in environmentally persistent free radicals and the generation of reactive radical species in humic substances, Front. Environ. Sci. Eng., 14, 1-10, 2020.

Shiraiwa, M., Ueda, K., Pozzer, A., Lammel, G., Kampf, C. J., Fushimi, A., Enami, S., Arangio, A. M., Fröhlich-Nowoisky, J., Fujitani, Y., Furuyama, A., Lakey, P. S. J., Lelieveld, J., Lucas, K., Morino, Y., Pöschl, U., Takahama, S., Takami, A., Tong, H., Weber, B., Yoshino, A., and Sato, K.: Aerosol health effects from molecular to global scales, Environ. Sci. Technol., 51, 13545-13567, 2017.

Shrivastava, M., Andreae, M. O., Artaxo, P., Barbosa, H. M., Berg, L. K., Brito, J., Ching, J., Easter, R. C., Fan, J., and Fast, J. D.: Urban pollution greatly enhances formation of natural aerosols over the Amazon rainforest, Nat. Commun., 10, 1046, 2019.

Sies, H., Berndt, C., and Jones, D. P.: Oxidative stress, Annu. Rev. Biochem., 86, 715-748, 2017.

Simic, M., Neta, P., and Hayon, E.: Pulse radiolysis study of alcohols in aqueous solution, J. Phys. Chem., 73, 3794-3800, 1969.

Singh, D. K., and Gupta, T.: Role of transition metals with water soluble organic carbon in the formation of secondary organic aerosol and metallo - organics in PM_1 sampled during post monsoon and pre-winter time, J. Aerosol Sci., 94, 56-69, 2016.

Su, H., Cheng, Y., and Pöschl, U.: New Multiphase Chemical Processes Influencing Atmospheric Aerosols, Air Quality, and Climate in the Anthropocene, Acc. Chem. Res., 53, 2034-2043, 2020.

Tan, J., Xiang, P., Zhou, X., Duan, J., Ma, Y., He, K., Cheng, Y., Yu, J., and Querol, X.: Chemical characterization of humic-like substances (HULIS) in $PM_{2.5}$ in Lanzhou, China, Sci. Total Environ., 573, 1481-1490, 2016.

Tang, W.-W., Zeng, G.-M., Gong, J.-L., Liang, J., Xu, P., Zhang, C., and Huang, B.-B.: Impact of humic/fulvic acid on the removal of heavy metals from aqueous solutions using nanomaterials: a review, Sci. Total Environ., 468, 1014-1027, 2014.

Tao, W., Su, H., Zheng, G., Wang, J., Wei, C., Liu, L., Ma, N., Li, M., Zhang, Q., and Pöschl, U.: Aerosol pH and chemical regimes of sulfate formation in aerosol water during winter haze in the North China Plain, Atmos. Chem. Phys., 20, 11729-11746, 2020.

Tong, H., Arangio, A. M., Lakey, P. S., Berkemeier, T., Liu, F., Kampf, C. J., Brune, W. H., Pöschl, U., and Shiraiwa, M.: Hydroxyl radicals from secondary organic aerosol decomposition in water, Atmos. Chem. Phys., 16, 1761-1771, 2016a.

Tong, H., Kourtchev, I., Pant, P., Keyte, I. J., O'Connor, I. P., Wenger, J. C., Pope, F. D., Harrison, R. M., and Kalberer, M.: Molecular composition of organic aerosols at urban background and road tunnel sites using ultra-high resolution mass spectrometry, Faraday Discuss., 189, 51-68, 2016b.

Tong, H., Lakey, P. S., Arangio, A. M., Socorro, J., Kampf, C. J., Berkemeier, T., Brune, W. H., Pöschl, U., and Shiraiwa, M.: Reactive oxygen species formed in aqueous mixtures of secondary organic aerosols and mineral dust influencing cloud chemistry and public health in the Anthropocene, Faraday Discuss., 200, 251-270, 2017.

Tong, H., Lakey, P. S., Arangio, A. M., Socorro, J., Shen, F., Lucas, K., Brune, W. H., Pöschl, U., and Shiraiwa, M.: Reactive oxygen species formed by secondary organic aerosols in water and surrogate lung fluid, Environ. Sci. Technol., 52, 11642-11651, 2018.

Tong, H., Zhang, Y., Filippi, A., Wang, T., Li, C., Liu, F., Leppla, D., Kourtchev, I., Wang, K., Keskinen, H.-M., Levula, J. T., Arangio, A. M., Shen, F., Ditas, F., Martin, S. T., Artaxo, P., Godoi, R. H. M., Yamamoto, C. I., Souza, R. A. F. d., Huang, R.-J., Berkemeier, T., Wang, Y., Su, H., Cheng, Y., Pope, F. D., Fu, P., Yao, M., Pöhlker, C., Petäjä, T., Kulmala, M., Andreae, M. O., Shiraiwa, M., Pöschl, U., Hoffmann, T., and Kalberer, M.: Radical Formation by Fine Particulate Matter Associated with Highly Oxygenated Molecules, Environ. Sci. Technol., 53, 12506-12518, 2019.

Tröstl, J., Chuang, W. K., Gordon, H., Heinritzi, M., Yan, C., Molteni, U., Ahlm, L., Frege, C., Bianchi, F., and Wagner, R.: The role of low-volatility organic compounds in initial particle growth in the atmosphere, Nature, 533, 527-531, 2016.

Tseitlin, M., Eaton, S. S., and Eaton, G. R.: Uncertainty analysis for absorption and first‐derivative electron paramagnetic resonance spectra, Concepts Magn. Reson., Part A, 40, 295-305, 2012.

Valavanidis, A., Salika, A., and Theodoropoulou, A.: Generation of hydroxyl radicals by urban suspended particulate air matter. The role of iron ions, Atmos. Environ., 34, 2379-2386, 2000.

Valavanidis, A., Fiotakis, K., Bakeas, E., and Vlahogianni, T.: Electron paramagnetic resonance study of the generation of reactive oxygen species catalysed by transition metals and quinoid redox cycling by inhalable ambient particulate matter, Redox. Rep., 10, 37-51, 2005.

Vejerano, E. P., Rao, G., Khachatryan, L., Cormier, S. A., and Lomnicki, S.: Environmentally persistent free radicals: Insights on a new class of pollutants, Environ. Sci. Technol., 52, 2468-2481, 2018.

Verma, V., Fang, T., Guo, H., King, L., Bates, J., Peltier, R., Edgerton, E., Russell, A., and Weber, R.: Reactive oxygen species associated with water-soluble $PM_{2.5}$ in the southeastern United States: spatiotemporal trends and source apportionment, Atmos. Chem. Phys., 14, 12915-12930, 2014.

Verma, V., Fang, T., Xu, L., Peltier, R. E., Russell, A. G., Ng, N. L., and Weber, R. J.: Organic aerosols associated with the generation of reactive oxygen species (ROS) by water-soluble $PM_{2.5}$, Environ. Sci. Technol., 49, 4646-4656, 2015.

Wang, C., Wang, Z., Peng, A., Hou, J., and Xin, W.: Interaction between fulvic acids of different origins and active oxygen radicals, Sci. China C Life Sci., 39, 267-275, 1996.

Wang, K., Zhang, Y., Huang, R.-J., Cao, J., and Hoffmann, T.: UHPLC-Orbitrap mass spectrometric characterization of organic aerosol from a central European city (Mainz, Germany) and a Chinese megacity (Beijing), Atmos. Environ., 189, 22-29, 2018a.

Wang, K., Zhang, Y., Huang, R.-J., Wang, M., Ni, H., Kampf, C. J., Cheng, Y., Bilde, M., Glasius, M., and Hoffmann, T.: Molecular characterization and source identification of atmospheric particulate organosulfates using ultrahigh resolution mass spectrometry, Environ. Sci. Technol., 53, 6192-6202, 2019.

Wang, N., Miller, C. J., Wang, P., and Waite, T. D.: Quantitative determination of trace hydrogen peroxide in the presence of sulfide using the Amplex Red/horseradish peroxidase assay, Anal. Chim. Acta, 963, 61-67, 2017.

Wang, S., Ye, J., Soong, R., Wu, B., Yu, L., Simpson, A. J., and Chan, A. W.: Relationship between chemical composition and oxidative potential of secondary organic aerosol from polycyclic aromatic hydrocarbons, Atmos. Chem. Phys., 18, 3987-4003, 2018b.

Wang, W., Liu, M., Wang, T., Song, Y., Zhou, L., Cao, J., Hu, J., Tang, G., Chen, Z., and Li, Z.: Sulfate formation is dominated by manganese-catalyzed oxidation of SO 2 on aerosol surfaces during haze events, Nat. Commun., 12, 1-10, 2021.

Wang, Y., Arellanes, C., Curtis, D. B., and Paulson, S. E.: Probing the source of hydrogen peroxide associated with coarse mode aerosol particles in Southern California, Environ. Sci. Technol., 44, 4070-4075, 2010.

Wang, Y., Hopke, P. K., Sun, L., Chalupa, D. C., and Utell, M. J.: Laboratory and field testing of an automated atmospheric particle-bound reactive oxygen species sampling-analysis system, J. Toxicol., 2011, 419476, 2011a.

Wang, Y., Kim, H., and Paulson, S. E.: Hydrogen peroxide generation from α-and β-pinene and toluene secondary organic aerosols, Atmos. Environ., 45, 3149-3156, 2011b.

Wang, Y., Arellanes, C., and Paulson, S. E.: Hydrogen peroxide associated with ambient fine-mode, diesel, and biodiesel aerosol particles in Southern California, Aerosol Sci. Technol., 46, 394-402, 2012.

Wang, Y., Hu, M., Guo, S., Wang, Y., Zheng, J., Yang, Y., Zhu, W., Tang, R., Li, X., and Liu, Y.: The secondary formation of organosulfates under interactions between biogenic emissions and anthropogenic pollutants in summer in Beijing, Atmos. Chem. Phys., 18, 10693-10713, 2018c.

Wei, J., Yu, H., Wang, Y., and Verma, V.: Complexation of Iron and Copper in Ambient Particulate Matter and Its Effect on the Oxidative Potential Measured in a Surrogate Lung Fluid, Environ. Sci. Technol., 53, 1661-1671, 2019.

Wei, J., Fang, T., Wong, C., Lakey, P. S., Nizkorodov, S. A., and Shiraiwa, M.: Superoxide Formation from Aqueous Reactions of Biogenic Secondary Organic Aerosols, Environ. Sci. Technol., 55, 260-270, 2021.

Win, M. S., Tian, Z., Zhao, H., Xiao, K., Peng, J., Shang, Y., Wu, M., Xiu, G., Lu, S., and Yonemochi, S.: Atmospheric HULIS and its ability to mediate the reactive oxygen species (ROS): A review, J. Environ. Sci., 71, 13-31, 2018.

Xia, T., Korge, P., Weiss, J. N., Li, N., Venkatesen, M. I., Sioutas, C., and Nel, A.: Quinones and aromatic chemical compounds in particulate matter induce mitochondrial dysfunction: implications for ultrafine particle toxicity, Environ. Health Perspect., 112, 1347-1358, 2004.

Xiong, Q., Yu, H., Wang, R., Wei, J., and Verma, V.: Rethinking dithiothreitol-based particulate matter oxidative potential: measuring dithiothreitol consumption versus reactive oxygen species generation, Environ. Sci. Technol., 51, 6507-6514, 2017.

Xu, L., Guo, H., Boyd, C. M., Klein, M., Bougiatioti, A., Cerully, K. M., Hite, J. R., Isaacman-VanWertz, G., Kreisberg, N. M., and Knote, C.: Effects of anthropogenic emissions on aerosol formation from isoprene and monoterpenes in the southeastern United States, Proc. Natl. Acad. Sci. U.S.A., 112, 37-42, 2015.

Yan, D., Cui, H., Zhu, W., Talbot, A., Zhang, L. G., Sherman, J. H., and Keidar, M.: The strong cell-based hydrogen peroxide generation triggered by cold atmospheric plasma, Sci. Rep., 7, 1-9, 2017.

Yang, R., Su, H., Qu, S., and Wang, X.: Capacity of humic substances to complex with iron at different salinities in the Yangtze River estuary and East China Sea, Sci. Rep., 7, 1381, 2017.

Yassine, M. M., Harir, M., Dabek‐Zlotorzynska, E., and Schmitt‐Kopplin, P.: Structural characterization of organic aerosol using Fourier transform ion cyclotron resonance mass spectrometry: aromaticity equivalent approach, Rapid Commun. Mass Spectrom., 28, 2445-2454, 2014.

Yu, H., Wei, J., Cheng, Y., Subedi, K., and Verma, V.: Synergistic and antagonistic interactions among the particulate matter components in generating reactive oxygen species based on the dithiothreitol assay, Environ. Sci. Technol., 52, 2261-2270, 2018.

Yun, X., Shen, G., Shen, H., Meng, W., Chen, Y., Xu, H., Ren, Y., Zhong, Q., Du, W., and Ma, J.: Residential solid fuel emissions contribute significantly to air pollution and associated health impacts in China, Sci. Adv., 6, eaba7621, 2020.

Zhang, Y., and Tao, S.: Global atmospheric emission inventory of polycyclic aromatic hydrocarbons (PAHs) for 2004, Atmos. Environ., 43, 812-819, 2009.

Zhao, H., Joseph, J., Zhang, H., Karoui, H., and Kalyanaraman, B.: Synthesis and biochemical applications of a solid cyclic nitrone spin trap: a relatively superior trap for detecting superoxide anions and glutathiyl radicals, Free Radic. Biol. Med., 31, 599-606, 2001.

Zheng, G., He, K., Duan, F., Cheng, Y., and Ma, Y.: Measurement of humic-like substances in aerosols: A review, Environ. Pollut., 181, 301-314, 2013.

Zheng, G., Su, H., Wang, S., Andreae, M. O., Pöschl, U., and Cheng, Y.: Multiphase buffer theory explains contrasts in atmospheric aerosol acidity, Science, 369, 1374-1377, 2020.

Zhou, J., Zotter, P., Bruns, E. A., Stefenelli, G., Bhattu, D., Brown, S., Bertrand, A., Marchand, N., Lamkaddam, H., and Slowik, J. G.: Particle-bound reactive oxygen species (PB-ROS) emissions and formation pathways in residential wood smoke under different combustion and aging conditions, Atmos. Chem. Phys., 18, 6985-7000, 2018.

Zuo, Y., and Hoigne, J.: Formation of hydrogen peroxide and depletion of oxalic acid in atmospheric water by photolysis of iron(III)-oxalato complexes, Environ. Sci. Technol., 26, 1014-1022, 1992.

Zuo, Y., and Deng, Y.: Iron (II)-catalyzed photochemical decomposition of oxalic acid and generation of H2O2 in atmospheric liquid phases, Chemosphere, 35, 2051-2058, 1997.

Data availability

The dataset for this paper is available upon request from the corresponding author (h.tong@mpic.de).

Supporting Information

Supporting material consists of seven figures and five tables.

Author contributions

HT and UP designed the esperiment and wrote up the original draft together with FL. CX, SY, and HK involved in the collection of ambient particles. HT, FL, AF, and YZ participated in laboratory measurements and data analysis. All other co-authors participated in results discussion and manuscript editing.

AUTHOR INFORMATION

Corresponding Author

Haijie Tong

Phone: (+852) 2766-6025

E-mail: h.tong@mpic.de; haijie.tong@polyu.edu.hk.

ORCID:

Haijie Tong: 0000-0001-9887-7836

Maosheng Yao: 0000-0002-1442-8054

Thomas Berkemeier: 0000-0001-6390-6465

Manabu Shiraiwa: 0000-0003-2532-5373

Ulrich Pöschl: 0000-0003-1412-35570000-0001-9887-7836

Competing interests

The authors declare no competing financial interest.

Acknowledgements

This work was funded by the Max Planck Society, ACTRIS, ECAC, the Finnish Centre of Excellence under Academy of Finland (projects no. 307331 and 272041), and PolyU (P0036313). Siegfried Herrmann and Steve Galer from Climate Geochemistry Department of Max Planck Institute for Chemistry are gratefully acknowledged for ICP-MS analysis. Technical staffs at SMEARII station are acknowledged for the impactor maintenance. MS acknowledges funding from the National Science Foundation (CHE-1808125).

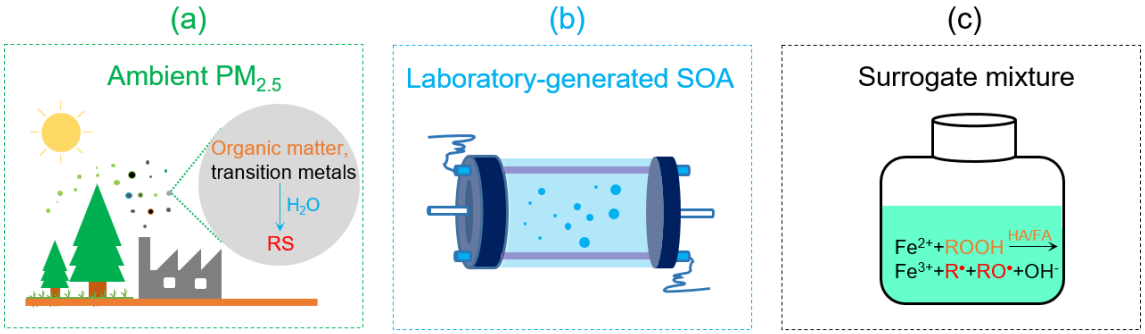

881

882 **Figure 1.** Schematic illustration of research approach and comparison of aqueous-phase reactive species
883 (RS) formed in aqueous extracts of ambient fine particulate matter ($PM_{2.5}$), and laboratory generated
884 secondary organic aerosols (SOA), and surrogate mixtures. ROOH: organic hydroperoxide. HA: humic
885 acid. FA: fulvic acid. $R^{\bullet}$ and $RO^{\bullet}$: C- and O-centered organic radicals, respectively.

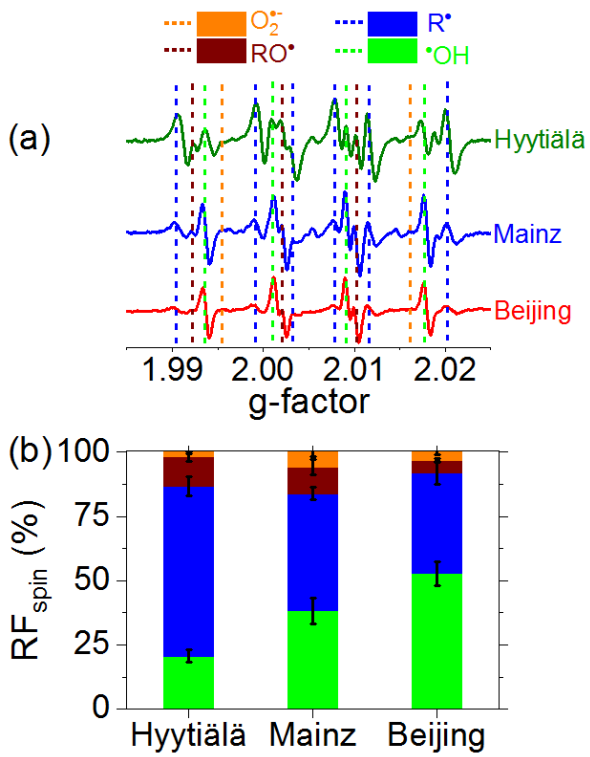

886

887 **Figure 2.** (a) Electron paramagnetic resonance (EPR) spectra and (b) relative fraction of unpaired electrons
888 (RF_{spin}) attributed to different types of radicals formed in aqueous extracts of ambient $PM_{2.5}$ from Hyytiälä,
889 Mainz, and Beijing. Dotted vertical lines in (a) indicate peak positions of different radical adducts. The
890 spectra intensity in (a), RF_{spin} values and error bars in (b) represent arithmetic mean values and standard
891 error (6-13 samples per location).

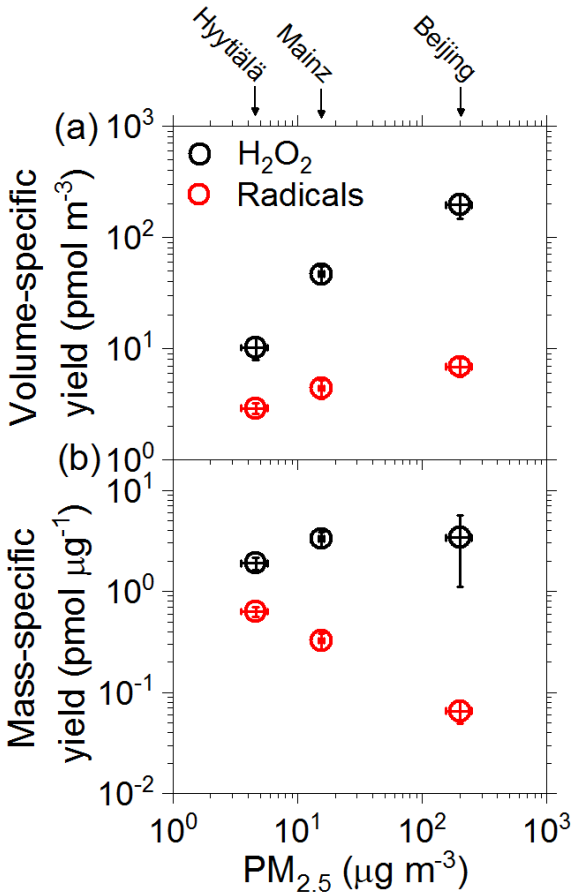

892

893 **Figure 3.** (a) Air sample volume-specific yields and (b) mass-specific yields of aqueous-phase radicals (◯)
894 and H_2O_2 (◯) formed in aqueous extracts of ambient $PM_{2.5}$ from Hyytiälä, Mainz, and Beijing. plotted
895 against $PM_{2.5}$ mass concentration. The error bars represent standard errors of the mean (4-12 samples per
896 location).

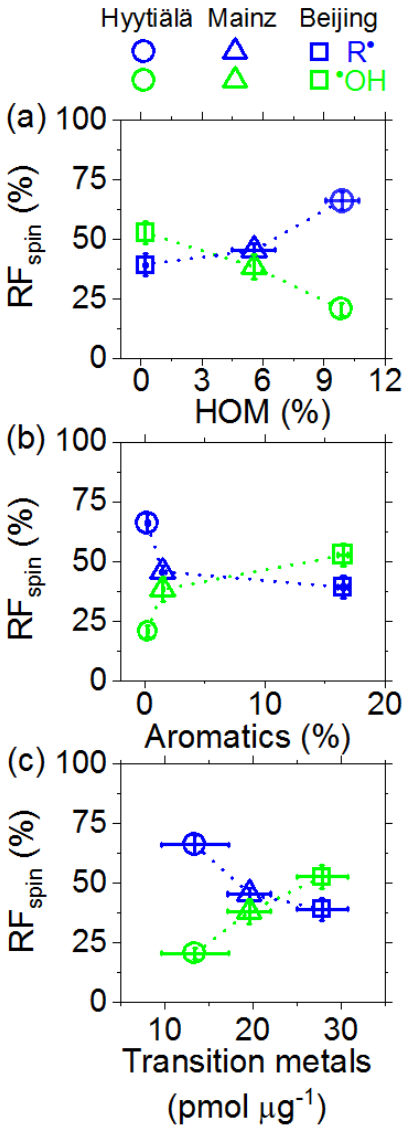

Figure 4. Relative fraction (RF_{spin}) of aqueous-phase C-centered (R•) and •OH radicals plotted against the relative abundance of (a) highly oxygenated organic molecules (HOM), (b) aromatics, and (c) water-soluble transition metals in ambient $PM_{2.5}$ from Hyytiälä, Mainz, and Beijing. The relative abundances of HOM and aromatics in (a-b) represent the sum chromatographic area of HOM or aromatics divided by the sum chromatographic area of all assigned organic compounds. The abundances of HOM in (a) were adopted from a recent companion study (Tong et al., 2019). The error bars represent standard errors of the mean (4 to 12 samples per location). The dashed lines are to guide the eye.

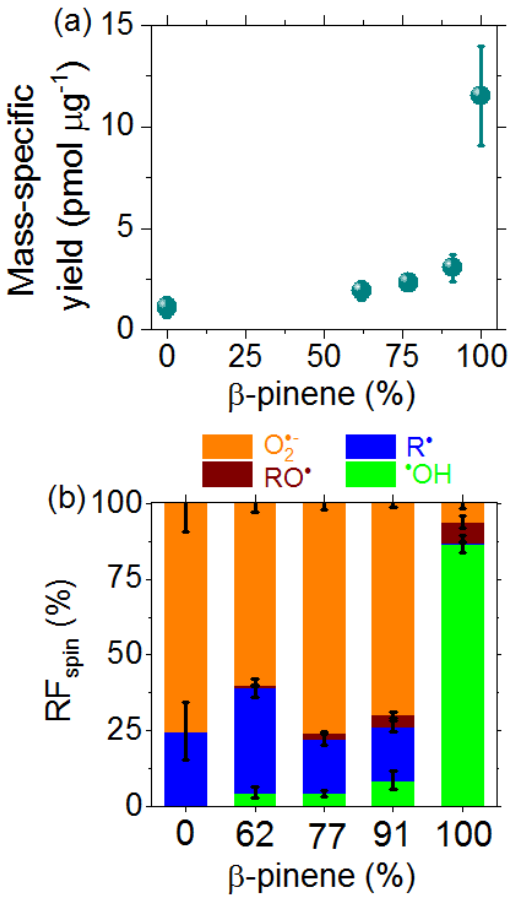

905

906 **Figure 5.** (a) Mass-specific yields and (b) relative fractions (RF_{spin}) of different types of radicals formed
907 upon aqueous extraction of laboratory-generated SOA from precursor mixtures of β-pinene and naphthalene
908 plotted against the mass fraction of β-pinene (%) in the precursor mixture. The error bars represent standard
909 errors (4-6 samples per data point).

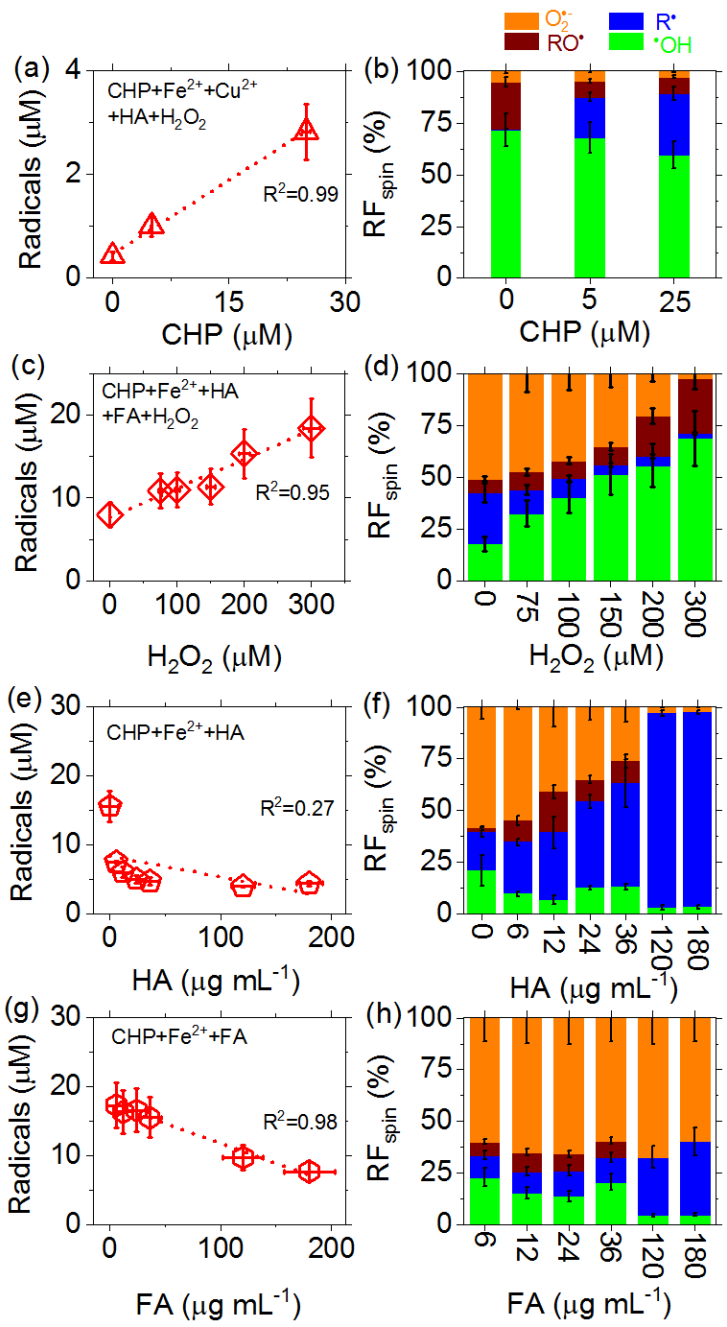

Figure 6. (a, c, e, g) Total concentrations and (b, d, f, h) relative fractions (RF_{spin}) of different types of radicals (spins) observed in aqueous mixtures of Fe^{2+}, Cu^{2+}, humic acid (HA), fulvic acid (FA), cumene hydroperoxide (CHP), and H_2O_2, serving as surrogate species for redox-active components of $PM_{2.5}$. (a, b): 0-25 μM CHP, 43 μM Fe^{2+}, 3 μM Cu^{2+}, 4 μg mL^{-1} HA, 7 μM H_2O_2 (CHP+Fe^{2+}+Cu^{2+}+HA+H_2O_2). (c, d): CHP: 100 μM. Fe^{2+}: 300 μM. HA: 100 μg mL^{-1}. FA: 80 μg mL^{-1}. H_2O_2: 0-300 μM. (e, f): 100 μM CHP, 300 μM Fe^{2+}, 0-180 μg mL^{-1} HA (CHP+Fe^{2+}+HA). (g, h): 100 μM CHP, 300 μM Fe^{2+}, 6-180 μg mL^{-1} FA (CHP+Fe^{2+}+FA). The error bars represent the uncertainties of EPR signal integration (y-axis) and solute concentration (x-axis), respectively.